

L^2 -ESTIMATES FOR THE DG IIPG-0 SCHEME

BLANCA AYUSO DE DIOS, FRANCO BREZZI, OTO HAVLE,
AND L. DONATELLA MARINI

ABSTRACT. We discuss the optimality in L^2 of a variant of the Incomplete Discontinuous Galerkin Interior Penalty method (IIPG) for second order linear elliptic problems. We prove optimal estimate, in two and three dimensions, for the lowest order case under suitable regularity assumptions on the data and on the mesh. We also provide numerical evidence, in one dimension, of the necessity of the regularity assumptions.

1. INTRODUCTION

Interior Penalty Discontinuous Galerkin methods for diffusion equations were introduced in the late seventies and in the beginning of the eighties (see [24] and [3]). They were not used for some time, but were revived in the late nineties, mostly in order to deal with the diffusive part of convection dominated problems.

At the beginning of the last decade, a considerable interest aroused for the use of nonsymmetric methods, even for discretizing symmetric operators as the Laplace operator. The interest was mainly addressed to the Baumann-Oden approach, in which the anti-symmetrization of the DG-consistency terms allowed a much simpler proof of a-priori estimates and stability results. Later on, other nonsymmetric approaches were proposed (in particular by Sun and Wheeler) based on encouraging numerical tests. The discrete- H^1 error estimates for all these methods are quite easy to prove, essentially using the same arguments used for dealing with the original symmetric scheme (then renamed “IP”, then renamed again “SIPG”). See for instance [4] and the references therein.

However, many questions remained open for the last ten years concerning the optimality of nonsymmetric methods in L^2 , even when considering the approximation of the simple Poisson problem. Indeed, on the one hand the classical Aubin-Nitsche duality technique for proving L^2 estimates cannot be applied, and on the other hand the numerical experiments are not always conclusive, as the quality of the results seems to depend heavily on *parity of the degree* of the local polynomials and/or on the regularity of the mesh and of the right-hand side.

In [17] the authors showed optimal error estimates for the NIPG approximation for the one-dimensional problem on uniform grids (for odd degrees). Still in one-dimension, in [13] a superconvergence result for the error in the derivative at Gauss-nodes is shown for the NIPG and SIPG, always for uniform grids and odd degrees. As a consequence, the author could easily deduce an improved $k + 1/2$

rate of convergence in the L^2 -norm for the NIPG method (for uniform meshes and k odd).

More recently, in [16] the authors provided numerical evidence of the sub-optimal convergence in L^2 of the NIPG approximation on some particular meshes (in 1D and in 2D) having some periodic pattern, while in [15] L^2 -optimality for the one-dimensional IIPG approximation is proved on locally quasi-uniform meshes. Furthermore, the authors establish some necessary conditions on the choice of the penalty parameter (depending on the lengths of the neighboring intervals and on the polynomial degree), for guaranteeing the L^2 -optimality for odd degrees.

Few results are known concerning the L^2 -optimality of non symmetric DG methods in several dimensions. In particular, results were obtained in [12] for a weakly-penalized piecewise linear NIPG with strongly imposed boundary conditions and strong regularity assumptions on the mesh (see Remarks 2.1, 4.1, and 5.1). In [23] optimal estimates were derived for the discretization of a parabolic problem with the lowest order NIPG and IIPG methods on uniform rectangular grids. For a comparison with our procedure see again Remark 5.1.

We also note that all the works providing some L^2 optimality results for non-symmetric DG schemes require stronger regularity assumptions (on the right-hand side and/or on the mesh) than those normally used for the L^2 -error analysis of symmetric schemes (based on the Aubin-Nitsche technique).

In the present paper we want to add some additional steps on these issues. For the sake of simplicity, we consider the following very simple model problem. Let Ω be a bounded, convex, polygonal domain in \mathbf{R}^d , $d \geq 2$, and let $f \in L^2(\Omega)$. We look for $u \in H^2(\Omega)$ such that

$$(1.1) \quad \begin{cases} -\Delta u = f & \text{in } \Omega, \\ u = 0 & \text{in } \Omega. \end{cases}$$

With the same techniques more general linear elliptic second order operators could be considered, as well as more general boundary conditions.

We will analyze the lowest order (i.e. piecewise linear discontinuous) approximation of the so called ‘‘Incomplete Interior Penalty Galerkin’’ method (IIPG) or, actually, a minor variant of it, penalizing only the mean value of the jumps (IIPG-0). We underline the fact that here we consider *weakly imposed* boundary conditions, as is typical and in some sense more natural for DG methods. For the IIPG-0 method we show that this can be done without introducing major difficulties in the estimates. For other methods (as NIPG or NIPG-0) optimal L^2 estimates, so far, can only be proved in the case of *strongly imposed* boundary conditions, where the variational formulation is restricted to piecewise polynomials that already satisfy the boundary condition, at least for the average on each boundary edge (face). See for instance [12] or our Remark 5.1 here below.

Our approach shares with previous works the idea of using a decomposition of the linear DG space (introduced in several dimensions in [12] and independently in [5] for the design of preconditioners).

We will show two types of L^2 -optimal error estimates for the IIPG-0 method with piecewise linear element. The first will require the use of *1-strongly regular meshes* (roughly speaking: decompositions where the measure of any two neighboring elements is one order smaller than the measure of the elements themselves), while the second will put requirements on the weights in the jump penalty terms (and, in three dimensions, also the quasi-uniformity of the mesh). In both cases our analysis will also require a better regularity of the right-hand side, namely, f in $H^1(\Omega) \cap L^\infty(\Omega)$. However (and this is an additional novelty presented in this paper) we demonstrate numerically that this “extra” regularity is indeed **necessary** for achieving the optimal order.

The outline of the paper is as follows. In Section 2 we describe the basic notation, we introduce the IIPG-0 method and revise some basic results that we need for the analysis. In Section 3 we report the error analysis in the energy norm. We study some further properties of the approximate solution to (1.1) in Section 4. In Section 5 we present the L^2 -error analysis of the IIPG-0 method on strongly regular meshes, and briefly discuss the extension to NIPG-0 in Remark 5.1, where we show that the results of [12] can be obtained here with less regularity assumptions on the mesh. In Section 6 we present the other approach to L^2 -error analysis of the IIPG-0 method, using more general meshes but stronger requirements on the penalty weights.

Finally, Section 7 contains some numerical examples validating the presented theory. In the last part of this section, we give numerical evidence showing that the regularity assumptions required by our analysis (and all previous ones) are indeed essential for achieving L^2 -optimality.

All over the paper, the inequality

$$A \lesssim B$$

will be used to indicate that there exists a constant C , depending only on the minimum angle of the decomposition, such that $A \leq C B$. We will also use standard notation of Sobolev spaces [1].

2. THE IIPG-0 METHOD

Let \mathcal{T}_h be a shape-regular family of decompositions of Ω into triangles T (or tetrahedrons if $d = 3$) without hanging nodes; let h_T denote the diameter of T , and

$$h = \max_{T \in \mathcal{T}_h} h_T.$$

Following [4], we recall the usual DG-tools. Let \mathcal{E}_h° be the set of interior edges (faces if $d = 3$), and let $e \in \mathcal{E}_h^\circ$ be shared by the elements T_1 and T_2 . Define the unit normal vectors \mathbf{n}_1^e and \mathbf{n}_2^e on e , external to T_1 and T_2 , respectively. For a function ζ , piecewise smooth on \mathcal{T}_h , using the notation $\zeta^i := \zeta|_{T_i}$ we define

averages and jumps as

$$\{\zeta\} = \frac{1}{2}(\zeta^1 + \zeta^2), \quad \llbracket \zeta \rrbracket = \zeta^1 \mathbf{n}_1^e + \zeta^2 \mathbf{n}_2^e \quad \text{on } e \in \mathcal{E}_h^\circ.$$

For a vector valued function $\boldsymbol{\tau}$, piecewise smooth on \mathcal{T}_h , with analogous meaning for $\boldsymbol{\tau}^1$ and $\boldsymbol{\tau}^2$, we define

$$\{\boldsymbol{\tau}\} = \frac{1}{2}(\boldsymbol{\tau}^1 + \boldsymbol{\tau}^2), \quad \llbracket \boldsymbol{\tau} \rrbracket = \boldsymbol{\tau}^1 \cdot \mathbf{n}_1^e + \boldsymbol{\tau}^2 \cdot \mathbf{n}_2^e \quad \text{on } e \in \mathcal{E}_h^\circ.$$

For $e \in \mathcal{E}_h^\partial$, the set of boundary edges, and \mathbf{n} =outward unit normal, we set

$$\llbracket \zeta \rrbracket = \zeta \mathbf{n}, \quad \{\zeta\} = \zeta, \quad \{\boldsymbol{\tau}\} = \boldsymbol{\tau}.$$

We shall also use the notation

$$\begin{aligned} (\nabla v, \nabla w)_{\mathcal{T}_h} &= \sum_{T \in \mathcal{T}_h} \int_T \nabla v \cdot \nabla w dx \\ \langle v, w \rangle_{\mathcal{E}_h} &= \sum_{e \in \mathcal{E}_h} \int_e v w d\ell \quad \forall v, w, \text{ piecewise smooth.} \end{aligned}$$

Let V^{DG} denote the discontinuous finite element space defined by:

$$(2.1) \quad V^{DG} := \{v \in L^2(\Omega) : v|_T \in \mathbb{P}^1(T) \forall T \in \mathcal{T}_h\},$$

where $\mathbb{P}^1(T)$ is the space of polynomials of degree ≤ 1 on T . We note that, in general, the functions in V^{DG} will have no limit for \mathbf{x} tending to any point of the interelement boundaries. Therefore, to start with, we shall consider that they are defined only in the interior of each element. For $m \geq 1$ we denote by $H^m(\mathcal{T}_h)$ the broken H^m space, that is, the space of functions belonging to $H^m(T)$ for all $T \in \mathcal{T}_h$. We set

$$V(h) := V^{DG} + H^2(\Omega) \cap H_0^1(\Omega) \subset H^2(\mathcal{T}_h)$$

and for $v \in V(h)$ we define the seminorms and norms

$$(2.2) \quad |v|_{1,h}^2 := \sum_{T \in \mathcal{T}_h} \|\nabla v\|_{0,T}^2 \quad | \llbracket v \rrbracket |_*^2 := \sum_{e \in \mathcal{E}_h} h_e^{-1} \|\llbracket v \rrbracket\|_{0,e}^2,$$

$$(2.3) \quad \| \llbracket v \rrbracket \|_*^2 := |v|_{1,h}^2 + | \llbracket v \rrbracket |_*^2 + \sum_{T \in \mathcal{T}_h} h_T^2 |v|_{2,T}^2,$$

(where h_e is the length of the edge e for $d = 2$ and the diameter of the face e for $d = 3$, and $|v|_{2,T}$ denotes the L^2 norm of the second derivatives). Occasionally, it might also be useful to separate the contribution to the norm $| \cdot |_*$ of internal and boundary edges, writing

$$| \llbracket v \rrbracket |_*^2 = \sum_{e \in \mathcal{E}_h^\circ} h_e^{-1} \|\llbracket v \rrbracket\|_{0,e}^2 + \sum_{e \in \mathcal{E}_h^\partial} h_e^{-1} \|\llbracket v \rrbracket\|_{0,e}^2 =: | \llbracket v \rrbracket |_{*, \mathcal{E}_h^\circ}^2 + | \llbracket v \rrbracket |_{*, \mathcal{E}_h^\partial}^2$$

The norm (2.3) is the natural one for obtaining boundedness of typical DG-bilinear forms in spaces like $V(h)$. On the other hand, the weaker norm

$$(2.4) \quad v \mapsto \|v\|_{DG} := (|v|_{1,h}^2 + \|\llbracket v \rrbracket_*\|^2)^{1/2}$$

is the natural one for analyzing the stability. Restricted to $v \in V^{DG}$, the norms (2.3) and (2.4) are equivalent, as is evident from a local inverse inequality. We also remark that both (2.3) and (2.4) define norms, not just seminorms, on $V(h)$. Indeed, the discrete Poincaré inequality given in [3], or [7], implies the existence of a constant C for which

$$\|v\|_0 \leq C(|v|_{1,h}^2 + \|\llbracket v \rrbracket_*\|^2)^{1/2} \quad \forall v \in V(h).$$

We recall the following trace inequality [2]

$$(2.5) \quad \|\varphi\|_{0,e}^2 \leq C_t(h_e^{-1}\|\varphi\|_{0,T}^2 + h_e|\varphi|_{1,T}^2) \quad \forall \varphi \in H^1(T),$$

where C_t is a constant depending only on the minimum angle of T . We observe that, denoting by K_e the union of elements having $e \in \mathcal{E}_h$ in common, the inequality (2.5) implies in particular

$$(2.6) \quad \|\llbracket \varphi \rrbracket\|_{0,e}^2 + \|\{\varphi\}\|_{0,e}^2 \leq 4C_t(h_e^{-1}\|\varphi\|_{0,K_e}^2 + h_e|\varphi|_{1,K_e}^2) \\ \forall \varphi \in H^1(\mathcal{T}_h) \quad \forall e \in \mathcal{E}_h.$$

We finally recall the useful formula

$$(2.7) \quad \sum_{T \in \mathcal{T}_h} \int_{\partial T} v \boldsymbol{\tau} \cdot \mathbf{n}_T = \sum_{e \in \mathcal{E}_h} \int_e \llbracket v \rrbracket \cdot \{\boldsymbol{\tau}\} + \sum_{e \in \mathcal{E}_h^\circ} \int_e \{v\} \llbracket \boldsymbol{\tau} \rrbracket.$$

We further introduce, for every $e \in \mathcal{E}_h$, a penalty weight S_e of the form

$$(2.8) \quad S_e = \alpha_e h_e^{-1} \quad \text{with } \alpha^{**} \geq \alpha_e \geq \alpha^* > 0, \quad \forall e \in \mathcal{E}_h,$$

where α^{**} and α^* are values fixed once and for all. We also consider the operator \mathcal{S} from $L^2(\mathcal{E}_h)$ into itself, defined on each $e \in \mathcal{E}_h$ as $(\mathcal{S}v)|_e = S_e v|_e$. We can then consider the IIPG bilinear form $\tilde{\mathcal{A}}(\cdot, \cdot)$, defined by (see [22]):

$$(2.9) \quad \tilde{\mathcal{A}}(v, w) = (\boldsymbol{\nabla} v, \boldsymbol{\nabla} w)_{\mathcal{T}_h} - \langle \{\boldsymbol{\nabla}_h v\}, \llbracket w \rrbracket \rangle_{\mathcal{E}_h} + \langle \mathcal{S} \llbracket v \rrbracket, \llbracket w \rrbracket \rangle_{\mathcal{E}_h}.$$

The IIPG approximation to the solution of (1.1) reads:

$$(2.10) \quad \text{find } \tilde{u}_h \in V^{DG} \quad \text{such that } \tilde{\mathcal{A}}(\tilde{u}_h, w) = (f, w)_{\mathcal{T}_h}, \quad \forall w \in V^{DG}.$$

It is well known (see e.g. [22] or [4]) that if α^* in (2.8) is *large enough* (depending of the minimum angle in the decomposition), then the bilinear form $\tilde{\mathcal{A}}(\cdot, \cdot)$ is coercive.

For each $e \in \mathcal{E}_h$ let $P_e^0 : L^2(e) \rightarrow \mathbb{P}^0(e)$ denote the L^2 -orthogonal projection onto constants. We denote by m_e the midpoint of the edge e or, in 3 dimensions, the barycenter of the face e . With an abuse of language, we will still call m_e

“midpoint”, and e “edge”, even in 3 dimensions. We note that from elementary integration rules we have

$$(2.11) \quad P_e^0(v) := \frac{1}{|e|} \int_e v dl = v(m_e), \quad \forall v \in \mathbb{P}^1(e),$$

where $|e|$ denotes the measure of e . We also consider the operator \mathcal{P} from $L^2(\mathcal{E}_h)$ into itself, that on each $e \in \mathcal{E}_h$ acts as P_e^0 . Using this projection we define the following bilinear form:

$$(2.12) \quad \mathcal{A}(v, w) = (\nabla v, \nabla w)_{\mathcal{T}_h} - \langle \{\nabla_h v\}, \llbracket w \rrbracket \rangle_{\mathcal{E}_h} + \langle \mathcal{S} \llbracket v \rrbracket, \mathcal{P}(\llbracket w \rrbracket) \rangle_{\mathcal{E}_h},$$

with \mathcal{S} defined as before. Note that the above bilinear form (2.12) is nothing but what results upon performing numerical integration (with the midpoint rule) in the bilinear form given in (2.9).

We also recall the following well known inequality, whose proof can be found, for instance, in [4]:

$$(2.13) \quad \int_e |v \{\nabla w\} \cdot \nu^e| dl \lesssim \left(\frac{\alpha_e}{h_e} \int_e v^2 dl \right)^{1/2} \left(\|w\|_{1, K_e}^2 + h_T |w|_{2, K_e}^2 \right)^{1/2} \quad \forall e \in \mathcal{E}_h,$$

where ν^e is a unit normal to e , and K_e is again the union of elements having e in common.

Using (2.12) we introduce the following variant of IIPG, that we call IIPG-0:

$$(2.14) \quad \text{find } u_h \in V^{DG} \text{ such that } \mathcal{A}(u_h, w) = (f, w)_{\mathcal{T}_h}, \quad \forall w \in V^{DG}$$

that will be the object of most of the analysis of the present paper. This type of IP discretization (also called *weakly penalized*) has been considered before by other authors (see for instance [8], [9], and [5]). We note that, following [10], $\mathcal{A}(\cdot, \cdot)$ can also be rewritten in the weighted residual framework as follows:

$$(2.15) \quad \mathcal{A}(v, w) = (-\Delta v, w)_{\mathcal{T}_h} + \langle \llbracket \nabla v \rrbracket, \{w\} \rangle_{\mathcal{E}_h^\circ} + \langle \mathcal{S} \llbracket v \rrbracket, \mathcal{P}(\llbracket w \rrbracket) \rangle_{\mathcal{E}_h},$$

$$\forall v, w \in V(h).$$

Remark 2.1. *Other variants of the original IIPG formulation (2.10) could be considered. For instance one could use the so-called **strong boundary conditions**, that amounts to use, instead of V^{DG} , the smaller space*

$$(2.16) \quad V_0^{DG} := \{v \in V^{DG} \text{ such that } P_e^0(v) = 0 \quad \forall e \in \mathcal{E}_h^\partial\}$$

*as done, for instance, in [12] for the NIPG method. Another possible variant would be to use a sort of **superpenalty** in the definition of the penalty weight S_e , taking in (2.8)*

$$S_e = \alpha h_e^{-p}$$

where p (instead of being 1 as in (2.8)) is bigger than 1, as done for instance in [8], [9]. Both variants are interesting, but somehow lack the traditional flavor of DG methods (moving them toward the more classical conforming or nonconforming Finite Element methods). Moreover, the use of superpenalty in advection-diffusion problems might deteriorate stability, and thus affect the performance of

the method for a range of local Péclet numbers. In other words, unless one has a specific need for these types of variants, “it’s not Cricket”.

3. ERROR ESTIMATES IN THE DG NORM

We now recall a result that will be used later on.

Lemma 3.1. *For $w \in H^1(\mathcal{T}_h)$ it holds*

$$(3.1) \quad |\mathcal{P}(\llbracket w \rrbracket)|_*^2 \leq |\llbracket w \rrbracket|_*^2 \lesssim (|w|_{1,h}^2 + |\mathcal{P}(\llbracket w \rrbracket)|_*^2) \equiv \llbracket w \rrbracket\llbracket_{DG}^2.$$

Proof. The result is well known (see for instance [11], or [5]). We sketch the proof for convenience of the reader. Equation (3.1) can be expanded to

$$\begin{aligned} \sum_{e \in \mathcal{E}_h} h_e^{-1} \|P_e^0(\llbracket w \rrbracket)\|_{0,e}^2 &\leq \sum_{e \in \mathcal{E}_h} h_e^{-1} \llbracket w \rrbracket\llbracket_{0,e}^2 \\ &\lesssim (|w|_{1,h}^2 + \sum_{e \in \mathcal{E}_h} h_e^{-1} \|P_e^0(\llbracket w \rrbracket)\|_{0,e}^2). \end{aligned}$$

The first inequality follows from the L^2 -boundedness of the projection \mathcal{P}_e^0 . For the second one, we observe that on each $e \subset \partial T$ and for each $\varphi \in H^1(T)$, adding an subtracting $P_e^0(\varphi)$, extending $P_e^0(\varphi)$ inside T , applying (2.5) and classical interpolation estimates we have

$$\begin{aligned} h_e^{-1} \|\varphi\|_{0,e}^2 &\leq h_e^{-1} \|\varphi - P_e^0(\varphi)\|_{0,e}^2 + h_e^{-1} \|P_e^0(\varphi)\|_{0,e}^2 \\ &\leq h_e^{-1} C_t (h_e^{-1} \|\varphi - P_e^0(\varphi)\|_{0,T}^2 + h_e |\varphi|_{1,T}^2) + h_e^{-1} \|P_e^0(\varphi)\|_{0,e}^2 \\ &\lesssim (|\varphi|_{1,T}^2 + h_e^{-1} \|P_e^0(\varphi)\|_{0,e}^2). \end{aligned}$$

Applying the above procedure to the jumps of w , as done for instance in (2.6), and summing over e we conclude the proof. \square

For the original IIPG approximation (2.10) optimal error estimates in the norm $\llbracket \cdot \rrbracket\llbracket_{DG}$ have been proved (see for instance [22]). For the solution of (2.14), optimal convergence in the DG norm can also be easily shown.

Theorem 3.2. *Let $u \in H^2(\Omega) \cap H_0^1(\Omega)$ be the solution of (1.1), and let u_h be the solution of (2.14). There exists a constant $\bar{\alpha} > 0$, depending only on the minimum angle of the decompositions, such that for every choice of \mathcal{S} with $\alpha^* \geq \bar{\alpha}$ we have*

$$(3.2) \quad \llbracket u - u_h \rrbracket\llbracket_{DG} \lesssim h \|u\|_{2,\Omega}.$$

Proof. Thanks to (3.1) and (2.13) one can easily check that there exist a constant C_b and (for α^* large enough) a constant C_s such that

$$\begin{aligned} \mathcal{A}(v, w) &\leq C_b \llbracket v \rrbracket\llbracket \llbracket w \rrbracket\llbracket \quad \forall v, w \in H^2(\mathcal{T}_h) \\ \mathcal{A}(v, v) &\geq C_s \llbracket v \rrbracket\llbracket_{DG}^2 \quad \forall v \in V^{DG}. \end{aligned}$$

Therefore, continuity and stability being satisfied, using standard arguments (see [4] for details), one can easily get the a-priori error estimate (3.2). \square

4. ADDITIONAL PROPERTIES OF THE DISCRETE SOLUTION

We shall discuss here some additional properties of the solution u_h of (2.14) that will be useful in proving L^2 error estimates.

For some of the results of the paper, we shall need to assume further regularity on the family of partitions \mathcal{T}_h . The next condition has been frequently used in the superconvergence analysis of conforming finite element methods (see for instance [18], [6]).

Definition: We say that a shape regular finite element partition \mathcal{T}_h is s -strongly regular if, for any pair of adjacent elements $T_1, T_2 \in \mathcal{T}_h$, the following condition is satisfied:

$$(4.1) \quad |T_1| - |T_2| \lesssim h^{d+s} \quad s > 0, \quad \forall T_1, T_2 \in \mathcal{T}_h \quad T_1 \cap T_2 \neq \emptyset.$$

We shall consider partitions that satisfy (4.1) with $s = 1$. Observe also that any shape regular partition satisfies (4.1) with $s = 0$.

Remark 4.1. *We explicitly point out that our parameter s does not coincide with the parameter ζ in the definition of asymptotically ζ -uniform decomposition in [12] that in our notation would become, instead of (4.1),*

$$|T_1| - |T_2| \lesssim h^{d+\zeta(d-1)}.$$

Hence, in a sense, $s = \zeta(d-1)$, though s and ζ play different roles in the error estimates (see Remark 5.1).

Following [5], we briefly review a decomposition of the space V^{DG} defined in (2.1), which will play a key role in our subsequent analysis.

In [12, 5] it was shown that

$$V^{DG} = V^{CR} \oplus \mathcal{Z},$$

where V^{CR} is the space of nonconforming piecewise linear elements (Crouzeix-Raviart), and \mathcal{Z} is a space of piecewise linear discontinuous elements having average with zero-meanvalue. More precisely:

$$(4.2) \quad \begin{aligned} V^{CR} &= \{v \in V^{DG} \text{ such that } \mathcal{P}(\llbracket v \rrbracket) = 0\}, \\ \mathcal{Z} &= \{z \in V^{DG} \text{ such that } \mathcal{P}_e^0(\{z\}) = 0 \forall e \in \mathcal{E}_h^\circ\}. \end{aligned}$$

Note that every function $\varphi \in V^{CR}$ has a finite limit at every midpoint m_e , so that we can assign the value

$$\varphi(m_e) := \lim_{\mathbf{x} \rightarrow \mathbf{m}_e} \varphi(\mathbf{x})$$

making the functions in V^{CR} continuous at the midpoints of internal edges (by virtue of (2.11)), and vanishing at the midpoints m_e of boundary edges. On the

other hand, every function $\psi \in \mathcal{Z}$ is such that $|\psi|$ has a finite limit at every midpoint m_e , so that we can give a meaning to the quantity

$$|\psi|(m_e) := \lim_{\mathbf{x} \rightarrow \mathbf{m}_e} |\psi(\mathbf{x})|,$$

and we note that

$$(4.3) \quad \llbracket \psi \rrbracket(m_e) = 2|\psi|(m_e) \quad \forall e \in \mathcal{E}_h^\circ, \quad \llbracket \psi \rrbracket(m_e) = |\psi|(m_e) \quad \forall e \in \mathcal{E}_h^\partial.$$

In a sense, the functions in \mathcal{Z} could be considered, somehow, as “high frequency”.

It is quite natural to choose for both spaces V^{CR} and \mathcal{Z} a basis associated to the midpoints of the edges. Let T be an element with edges e_i , and corresponding midpoints m_{e_i} , $i = 1, \dots, d+1$. To T we associate $d+1$ basis functions satisfying (see Fig. 4.1)

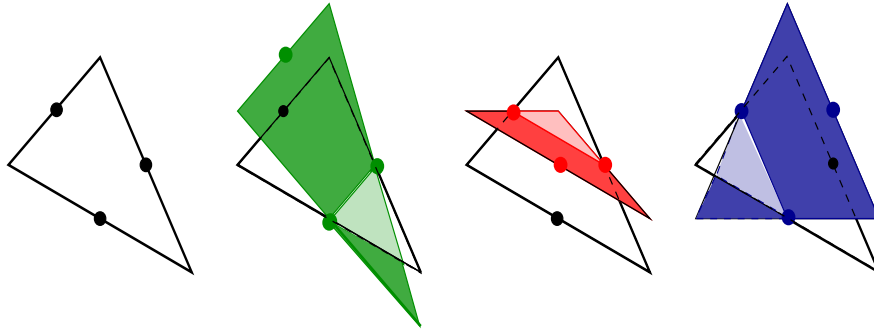


FIGURE 4.1. Local basis functions

$$\chi_T^{e_i}(x) \in \mathbb{P}^1(T) : \quad \chi_T^{e_i}(m_{e_j}) = \delta_{ij} \quad i, j = 1, \dots, d+1,$$

and being identically zero outside T . For any $e \in \mathcal{E}_h^\circ$, $e = \partial T_1 \cap \partial T_2$, we define

$$\varphi^e(x) = \chi_{T_1}^e(x) + \chi_{T_2}^e(x).$$

Note that the limit of φ^e , at every point of e , will be equal to 1 (see Fig. 4.2, right), so that

$$\{\varphi^e\}|_e = 1, \quad \llbracket \varphi^e \rrbracket|_e = 0.$$

For any edge $e \in \mathcal{E}_h^\circ$, $e = \partial T_1 \cap \partial T_2$, we denote by $\boldsymbol{\nu}^e$ one of the two normal directions, chosen once and for all. For $e \in \mathcal{E}_h^\partial$ we take instead $\boldsymbol{\nu}^e = \mathbf{n}_T^e = \mathbf{n}$. We note that, by simple computation, for every $e \in \mathcal{E}_h$ and for every $T \in \mathcal{T}_h$ with $e \subset \partial T$ we have

$$(4.4) \quad (\mathbf{n}_T^e \cdot \boldsymbol{\nu}^e) \boldsymbol{\nu}^e = \mathbf{n}_T^e$$

that we are going to use later on.

We then define, for any edge $e \in \mathcal{E}_h$, $e = \partial T_1 \cap \partial T_2$:

$$(4.5) \quad \psi^e(x) = \chi_{T_1}^e(x) \mathbf{n}_1^e \cdot \boldsymbol{\nu}^e + \chi_{T_2}^e(x) \mathbf{n}_2^e \cdot \boldsymbol{\nu}^e,$$

and for $e \in \mathcal{E}_h^\partial$, $e \subset \partial T$, we take

$$(4.6) \quad \psi^e(x) = \chi_T^e(x).$$

If e is an edge of $T \in \mathcal{T}_h$ we will have therefore

$$(4.7) \quad \psi_T^e = \chi_T^e(\mathbf{n}_T \cdot \boldsymbol{\nu}^e)$$

We note also that for every $e \in \mathcal{E}_h^\circ$ we have (see Fig. 4.2, left),

$$(4.8) \quad \{\psi^e\}_{|e} = 0, \quad |\psi^e|_{|e} = 1, \quad \llbracket \psi^e \rrbracket_{|e} = 2\boldsymbol{\nu}^e,$$

while for $e \in \mathcal{E}_h^\partial$

$$(4.9) \quad \psi^e|_e = 1, \quad \llbracket \psi^e \rrbracket_{|e} = \mathbf{n}.$$

Several other properties of the basis functions ψ^e will be useful in the sequel.

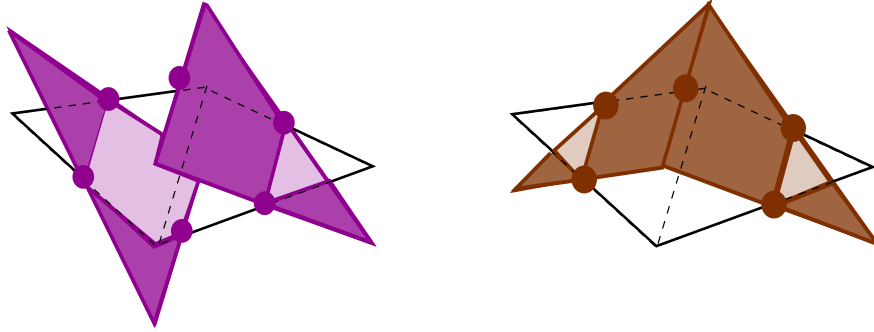


FIGURE 4.2. Global basis functions of \mathcal{Z} (left) and V^{CR} (right)

To start with, we note that from (4.7) we have¹ for every $e \in \mathcal{E}_h$ and for every $T \in \mathcal{T}_h$ with $e \subset \partial T$

$$(4.10) \quad \int_T \psi^e dx = \frac{|T|}{d+1} \mathbf{n}_T \cdot \boldsymbol{\nu}^e, \quad \int_T |\psi^e|^2 dx = C_d |T|.$$

From (4.10) and the shape regularity of the decomposition we will then have

$$(4.11) \quad \left| \int_T \psi^e dx \right| \lesssim h_e^d \quad \int_T |\psi^e|^2 dx \lesssim h_e^d.$$

We observe that in $L^2(\Omega)$ the functions χ_T^e , φ^e , and ψ^e are orthogonal bases for V^{DG} , V^{CR} , and \mathcal{Z} , respectively.

We finally point out that for the functions $z \in \mathcal{Z}$, together with (3.1), we have some additional properties, shown in the following lemma.

¹Using barycentric coordinates it is easy to check $\chi_T^{e_i} = 1 - d\lambda_i$, $i = 0, \dots, d+1$, with $\lambda_i \in \mathbb{P}^1(T)$ the basis function associated to the vertex of T opposite to e_i . Direct integration then yields to $C_d = \frac{d^2-d+2}{d^2+3d+2}$.

Lemma 4.2. *For every $z \in \mathcal{Z}$ we have*

$$|z|_{1,h}^2 \lesssim \sum_{e \in \mathcal{E}_h} h_e^{-2} \|z\|_{0,K_e}^2 \simeq |\mathcal{P}(\llbracket z \rrbracket)|_*^2,$$

where K_e is the union of the elements of \mathcal{T}_h having e as an edge (or “face” in 3 dimensions).

Proof. The first inequality follows from the usual inverse inequality. For the second we just recall the orthogonality in $L^2(\Omega)$ of the basis functions ψ^e and note that, denoting by $|z_e|$ the value of $|z|$ at the midpoint m_e of each $e \in \mathcal{E}_h$, we have:

$$\sum_{e \in \mathcal{E}_h} h_e^{-2} \|z\|_{0,K_e}^2 \simeq \sum_{e \in \mathcal{E}_h} h_e^{-2} |z_e|^2 \|\psi^e\|_{0,K_e}^2 \simeq \sum_{e \in \mathcal{E}_h} h_e^{-1} |z_e|^2 |e| \simeq |\mathcal{P}(\llbracket z \rrbracket)|_*^2$$

where in the last step we also used (4.3). \square

The following result can be found in [5] (see also [12]).

Proposition 4.3. *For any $v \in V^{DG}$ there exist a unique $v^{cr} \in V^{CR}$ and a unique $v^z \in \mathcal{Z}$ such that $v = v^{cr} + v^z$. Moreover, the following properties hold for the bilinear form (2.12):*

$$\begin{aligned} \mathcal{A}(v^{cr}, v^z) &= 0 \quad \forall v^{cr} \in V^{CR}, \quad \forall v^z \in \mathcal{Z}, \\ \mathcal{A}(v^{cr}, w^{cr}) &= (\nabla v^{cr}, \nabla w^{cr})_{\mathcal{T}_h} \quad \forall v^{cr}, w^{cr} \in V^{CR}, \\ \mathcal{A}(v^z, v^{cr}) &= (\nabla v^z, \nabla v^{cr})_{\mathcal{T}_h} \quad \forall v^z \in \mathcal{Z}, \quad \forall v^{cr} \in V^{CR}, \\ \mathcal{A}(v^z, w^z) &= \langle \mathcal{S}[\llbracket v^z \rrbracket], \mathcal{P}(\llbracket w^z \rrbracket) \rangle_{\mathcal{E}_h} \quad \forall v^z, w^z \in \mathcal{Z}. \end{aligned}$$

Proof (Sketch). The uniqueness of the decomposition follows by looking at the basis functions. The second and third equalities simply follow from (2.12) using the properties of functions in V^{CR} and \mathcal{Z} . The first and fourth follow from (2.15) using again the properties of V^{CR} and \mathcal{Z} . \square

As a consequence of Proposition 4.3, problem (2.14) can be written as:

$$(4.12) \quad \begin{cases} \text{Find } u_h = u^{cr} + u^z \text{ such that:} \\ i) \quad \langle \mathcal{S}[\llbracket u^z \rrbracket], \mathcal{P}(\llbracket v^z \rrbracket) \rangle_{\mathcal{E}_h} = (f, v^z)_{\mathcal{T}_h} \quad \forall v^z \in \mathcal{Z} \\ ii) \quad (\nabla u^{cr}, \nabla v^{cr})_{\mathcal{T}_h} = (f, v^{cr})_{\mathcal{T}_h} - (\nabla u^z, \nabla v^{cr})_{\mathcal{T}_h} \quad \forall v^{cr} \in V^{CR} \end{cases}$$

Observe that this last result implies that the solution of (2.14) reduces to solve two smaller and decoupled subproblems, one after the other.

The next Lemma provides a useful estimate, based on the fact that the linear system associated with (4.12) *i)* is diagonal.

Lemma 4.4. *Let $\Omega \subset \mathbb{R}^d$, $d \geq 1$, let $f \in L^2(\Omega)$, and let $u_h \in V_h^{DG}$ be the solution of (2.14). Let $u^{cr} \in V^{CR}$ and $u^z \in \mathcal{Z}_h$ be such that $u_h = u^{cr} + u^z$. Then we have*

$$\frac{2\alpha_e|e|}{h_e} \llbracket u^z \rrbracket(m_e) \cdot \boldsymbol{\nu}^e = \int_{\Omega} f \psi^e dx \quad \forall e \in \mathcal{E}_h^\circ;$$

$$\frac{\alpha_e|e|}{h_e} \llbracket u^z \rrbracket(m_e) \cdot \mathbf{n} = \frac{\alpha_e|e|}{h_e} u^z(m_e) = \int_{\Omega} f \psi^e dx \quad \forall e \in \mathcal{E}_h^\partial,$$

where ψ^e is the basis function associated to the edge e as defined in (4.5)-(4.6).

Proof. The proof follows immediately from (4.12) *i*), taking $v^z = \psi^e$ and using (2.8) together with the properties of the basis functions of \mathcal{Z} ; (4.8), and (4.9). \square

It is clear, from the above result, that it will be convenient to estimate quantities like

$$\int_{\Omega} f \psi^e dx$$

where f is a smooth enough function and ψ^e is one of the basis functions of \mathcal{Z} , associated to an edge e .

(i): If f is constant and \mathcal{T}_h is uniform, then

$$\int_{\Omega} f \psi^e dx = 0 \quad \forall e \in \mathcal{E}_h^\circ$$

since ψ^e is antisymmetric with respect to the edge e .

(ii): For $f \in H^1(\Omega)$, if \mathcal{T}_h is uniform, for all $e \in \mathcal{E}_h^\circ$ setting $K_e := \text{supp}(\psi^e)$ and $\bar{f} :=$ average of f over K_e we get

$$\left| \int_{\Omega} f \psi^e dx \right| = \left| \int_{K_e} (f - \bar{f}) \psi^e dx \right| \lesssim h_e \|f\|_{1,K_e} \|\psi^e\|_{0,K_e} \lesssim h_e^{1+d/2} \|f\|_{1,K_e}.$$

(iii): For $f \in H^1(\Omega) \cap L^\infty(\Omega)$, if \mathcal{T}_h is s -strongly-regular, with $s > 0$ as defined in (4.1), then for all $e \in \mathcal{E}_h^\circ$, denoting by T_1 and T_2 the elements having e in common, we have

$$\begin{aligned} (4.13) \quad \left| \int_{\Omega} f \psi^e dx \right| &= \left| \int_{K_e} (f - \bar{f}) \psi^e dx + \int_{K_e} \bar{f} \psi^e dx \right| \\ &\lesssim h_e^{1+d/2} \|f\|_{1,K_e} + \|f\|_{0,\infty,K_e} \left| |T_1| - |T_2| \right| \\ &\lesssim h_e^{1+d/2} \|f\|_{1,K_e} + h_e^{d+s} \|f\|_{0,\infty,\Omega}. \end{aligned}$$

(iv): For $f \in L^\infty(\Omega)$, for all $e \in \mathcal{E}_h^\partial$ and always with $K_e := \text{supp}(\psi^e)$, we have

$$(4.14) \quad \left| \int_{\Omega} f \psi^e dx \right| \lesssim |K_e| \|f\|_{0,\infty,K_e} \lesssim h_e^d \|f\|_{0,\infty,\Omega}.$$

We collect in particular the results (4.13), for $s = 1$, and (4.14) in the following theorem, that we are going to use for the L^2 error estimates.

Theorem 4.5. *Let $\Omega \subset \mathbb{R}^d, d \geq 1$, let $f \in H^1(\Omega) \cap L^\infty(\Omega)$, and let \mathcal{T}_h be an s -strongly regular finite element partition of Ω , as defined in (4.1). Let moreover $u_h = u^{cr} + u^z$ be the solution of (4.12). Then we have*

$$(4.15) \quad |\mathcal{P}(\llbracket u^z \rrbracket)|_{*, \mathcal{E}_h^\circ}^2 = \sum_{e \in \mathcal{E}_h^\circ} \frac{|e|}{h_e} |\llbracket u^z \rrbracket(m_e)|^2 \lesssim h^4 \|f\|_{1, \Omega}^2 + h^{2+2s} \|f\|_{0, \infty, \Omega}^2,$$

and for boundary edges:

$$(4.16) \quad \|\mathcal{P}(\llbracket u^z \rrbracket)\|_{0, \partial\Omega}^2 = \sum_{e \in \mathcal{E}_h^\partial} |e| |u^z(m_e)|^2 \lesssim h^4 \|f\|_{0, \infty, \Omega}^2.$$

Proof. The proof of (4.15) is immediate, using (4.13) from Lemma 4.4 and the fact that $\sum_{e \in \mathcal{E}_h^\circ} h_e^d \simeq |\Omega|$ and $|e| \simeq h_e^{d-1}$:

$$\begin{aligned} \sum_{e \in \mathcal{E}_h^\circ} \frac{|e|}{h_e} |\llbracket u^z \rrbracket(m_e)|^2 &= \sum_{e \in \mathcal{E}_h^\circ} \left(\frac{|e|}{h_e} |\llbracket u^z \rrbracket(m_e)| \right)^2 \frac{h_e}{|e|} \\ &\lesssim \sum_{e \in \mathcal{E}_h^\circ} \left(\frac{|e|}{h_e} |\llbracket u^z \rrbracket(m_e)| \right)^2 h_e^{2-d} \\ &\lesssim \sum_{e \in \mathcal{E}_h^\circ} h_e^{2-d} h_e^{2+d} \|f\|_{1, K_e}^2 + \sum_{e \in \mathcal{E}_h^\circ} h_e^{2-d} h_e^{2d+2s} \|f\|_{0, \infty, K_e}^2 \\ &\lesssim h^4 \sum_{e \in \mathcal{E}_h^\circ} \|f\|_{1, K_e}^2 + h_e^{2+2s} \|f\|_{0, \infty, \Omega}^2 \sum_{e \in \mathcal{E}_h^\circ} h_e^d \\ &\lesssim h^4 \|f\|_{1, \Omega}^2 + h^{2+2s} \|f\|_{0, \infty, \Omega}^2, \end{aligned}$$

while the proof of (4.16) uses (4.14) again from Lemma 4.4 and the fact that $\sum_{e \in \mathcal{E}_h^\partial} h_e^{d-1} \simeq |\partial\Omega|$:

$$\begin{aligned} \sum_{e \in \mathcal{E}_h^\partial} |e| |\llbracket u^z \rrbracket(m_e)|^2 &= \sum_{e \in \mathcal{E}_h^\partial} \left(\frac{|e|}{h_e} |\llbracket u^z \rrbracket(m_e)| \right)^2 \frac{h_e^2}{|e|} \\ &\lesssim \sum_{e \in \mathcal{E}_h^\partial} \left(\frac{|e|}{h_e} |\llbracket u^z \rrbracket(m_e)| \right)^2 h_e^{3-d} \\ &\lesssim \sum_{e \in \mathcal{E}_h^\partial} h_e^{3-d} h_e^{2d} \|f\|_{0, \infty, \Omega}^2 \\ &\lesssim h^4 \|f\|_{0, \infty, \Omega}^2 \sum_{e \in \mathcal{E}_h^\partial} h_e^{d-1} \lesssim h^4 \|f\|_{0, \infty, \Omega}^2. \quad \square \end{aligned}$$

Remark 4.6. *When using strong boundary conditions (see (2.16)), the estimate (4.15) would easily imply*

$$(4.17) \quad \| \|u^z\| \|_{DG} \lesssim h^2 \|f\|_{1,\Omega} + h^{1+s} \|f\|_{0,\infty,\Omega}.$$

On the other hand, for our case, combining (4.15) and (4.16) one does not get anything better than

$$(4.18) \quad \| \|u^z\| \|_{DG} \lesssim (h^{\frac{3}{2}} + h^{1+s}) (\|f\|_{1,\Omega}^2 + \|f\|_{0,\infty,\Omega}^2)^{1/2}.$$

5. L^2 -ERROR ANALYSIS ON STRONGLY REGULAR GRIDS

Theorem 5.1. *Let $\Omega \subset \mathbb{R}^d$, $d \geq 1$ be a convex domain. Let $f \in H^1(\Omega)$ and let u be the solution of the Poisson problem (1.1). Let \mathcal{T}_h be an s -strongly regular finite element partition of Ω , as defined in (4.1), and let $u_h \in V_h^{DG}$ be the solution of (2.14) (or, equivalently, of (4.12)). Then, the following error estimate holds*

$$(5.1) \quad \|u - u_h\|_{0,\Omega} \lesssim (h^2 + h^{1+s}) (\|f\|_{1,\Omega}^2 + \|f\|_{0,\infty,\Omega}^2)^{1/2}.$$

Proof. We proceed by standard duality arguments. Let $\psi \in H^2(\Omega) \cap H_0^1(\Omega)$ be the solution of the dual problem

$$-\Delta \psi = u - u_h \quad \text{in } \Omega, \quad \psi = 0 \quad \text{on } \partial\Omega.$$

The convexity of the domain Ω guarantees that the solution ψ satisfies the a-priori estimate

$$\|\psi\|_{2,\Omega} \lesssim \|u - u_h\|_{0,\Omega}.$$

Let ψ^I be the continuous piecewise linear interpolant of ψ . Standard approximation properties guarantee that (see [14]):

$$(5.2) \quad \|\psi - \psi^I\|_{0,\Omega} + h|\psi - \psi^I|_{1,h} \lesssim h^2 \|\psi\|_{2,\Omega} \lesssim \|u - u_h\|_{0,\Omega},$$

as well as

$$(5.3) \quad \left\| \frac{\partial \psi^I}{\partial \mathbf{n}} \right\|_{0,\partial\Omega} \lesssim \|\psi\|_{2,\Omega} \lesssim \|u - u_h\|_{0,\Omega}.$$

We also observe that Galerkin orthogonality, the definition (2.12) and $[\![\psi^I]\!] = 0$, imply

$$(5.4) \quad \mathcal{A}(u - u_h, \psi^I) \equiv (\nabla(u - u_h), \nabla \psi^I)_{\mathcal{T}_h} = 0.$$

Using the definition of the L^2 -norm, integrating by parts, using (2.7) and the regularity of ψ , then adding and subtracting ψ^I and using (5.4), and finally separating internal and boundary edges, we have

$$(5.5) \quad \begin{aligned} \|u - u_h\|_{0,\Omega}^2 &= (u - u_h, u - u_h)_{\mathcal{T}_h} = (u - u_h, -\Delta \psi)_{\mathcal{T}_h} \\ &= (\nabla(u - u_h), \nabla \psi)_{\mathcal{T}_h} - \langle \llbracket u - u_h \rrbracket, \{\nabla \psi\} \rangle_{\mathcal{E}_h} - \langle \{u - u_h\}, \llbracket \nabla \psi \rrbracket \rangle_{\mathcal{E}_h^\circ} \\ &= (\nabla(u - u_h), \nabla \psi)_{\mathcal{T}_h} - \langle \llbracket u - u_h \rrbracket, \{\nabla \psi\} \rangle_{\mathcal{E}_h} \\ &= (\nabla(u - u_h), \nabla(\psi - \psi^I))_{\mathcal{T}_h} - \langle \llbracket u - u_h \rrbracket, \{\nabla(\psi - \psi^I)\} \rangle_{\mathcal{E}_h} \end{aligned}$$

$$\begin{aligned}
 & - \langle \llbracket u - u_h \rrbracket, \{\nabla \psi^I\} \rangle_{\mathcal{E}_h} \\
 = & (\nabla(u - u_h), \nabla(\psi - \psi^I))_{\mathcal{T}_h} - \langle \llbracket u - u_h \rrbracket, \{\nabla(\psi - \psi^I)\} \rangle_{\mathcal{E}_h} \\
 & - \langle \llbracket u - u_h \rrbracket, \{\nabla \psi^I\} \rangle_{\mathcal{E}_h^\circ} - \langle \llbracket u - u_h \rrbracket, \{\nabla \psi^I\} \rangle_{\mathcal{E}_h^\partial} \\
 = &: I + II + III + IV.
 \end{aligned}$$

We then get, using Cauchy-Schwarz, (3.2), and (5.2):

$$\begin{aligned}
 |I| & := |(\nabla(u - u_h), \nabla(\psi - \psi^I))_{\mathcal{T}_h}| \leq |u - u_h|_{1,h} |\psi - \psi^I|_{1,h} \\
 (5.6) \quad & \lesssim h^2 \|u - u_h\|_{0,\Omega}.
 \end{aligned}$$

On the other hand, using (2.13), (3.2), and (5.2):

$$\begin{aligned}
 |II| & := |\langle \llbracket u - u_h \rrbracket, \{\nabla(\psi - \psi^I)\} \rangle_{\mathcal{E}_h}| \\
 (5.7) \quad & \lesssim \|\llbracket u - u_h \rrbracket\|_* (\|\psi - \psi^I\|_{1,h}^2 + h^2 |\psi - \psi^I|_{2,h}^2)^{1/2} \lesssim h^2 \|u - u_h\|_{0,\Omega}.
 \end{aligned}$$

To deal with III and IV we note first that $\llbracket u \rrbracket = 0$. Next, since $\{\nabla \psi^I\}$ is constant, $\llbracket u_h \rrbracket$ can be replaced by $\mathcal{P}(\llbracket u_h \rrbracket)$. Moreover, $\mathcal{P}(\llbracket u_h \rrbracket) = \mathcal{P}(\llbracket u^{cr} + u^z \rrbracket) = \mathcal{P}(\llbracket u^z \rrbracket)$ since, by definition (4.2) of V^{CR} , $\mathcal{P}(\llbracket u^{cr} \rrbracket) \equiv 0$. Hence:

$$(5.8) \quad III + IV = -\langle \mathcal{P}(\llbracket u^z \rrbracket), \{\nabla \psi^I\} \rangle_{\mathcal{E}_h^\circ} - \langle \mathcal{P}(\llbracket u^z \rrbracket), \{\nabla \psi^I\} \rangle_{\mathcal{E}_h^\partial}.$$

We then estimate III using (2.13), (4.15), and (5.2)

$$\begin{aligned}
 |III| & = |\langle \mathcal{P}(\llbracket u^z \rrbracket), \{\nabla \psi^I\} \rangle_{\mathcal{E}_h^\circ}| = \left| \sum_{e \in \mathcal{E}_h^\circ} \int_e \llbracket u^z \rrbracket(m_e) \{\nabla \psi^I\} d\ell \right| \\
 & \lesssim \left(\sum_{e \in \mathcal{E}_h^\circ} \frac{|e|}{h_e} |\llbracket u^z \rrbracket(m_e)|^2 \right)^{1/2} \left(\sum_{T \in \mathcal{T}_h} \|\psi^I\|_{1,T}^2 \right)^{1/2} \\
 & \lesssim |\mathcal{P}(\llbracket u^z \rrbracket)|_{*, \mathcal{E}_h^\circ}^2 \|\psi^I\|_{1,\Omega} \\
 (5.9) \quad & \lesssim (h^2 + h^{1+s}) (\|f\|_{1,\Omega}^2 + \|f\|_{0,\infty,\Omega}^2)^{1/2} \|\psi^I\|_{1,\Omega} \lesssim h^2 \|u - u_h\|_{0,\Omega},
 \end{aligned}$$

and IV using (4.16) and (5.3)

$$\begin{aligned}
 |IV| & = |\langle \mathcal{P}(\llbracket u^z \rrbracket), \{\nabla \psi^I\} \rangle_{\mathcal{E}_h^\partial}| \lesssim \|\mathcal{P}(\llbracket u^z \rrbracket)\|_{0,\partial\Omega} \left\| \frac{\partial \psi^I}{\partial \mathbf{n}} \right\|_{0,\partial\Omega} \\
 (5.10) \quad & \lesssim h^2 \|f\|_{0,\infty,\Omega} \left\| \frac{\partial \psi^I}{\partial \mathbf{n}} \right\|_{0,\partial\Omega} \lesssim h^2 \|u - u_h\|_{0,\Omega}.
 \end{aligned}$$

Collecting (5.6) –(5.10) we conclude the estimate. \square

Remark 5.1. *The above approach could also be applied to deal with the NIPG-0 scheme (see e.g. [12]). We recall that the NIPG-0 scheme could be written as: find $u_h \in V^{DG}$ such that*

$$(5.11) \quad \mathcal{A}^N(u_h, w) = (f, w)_{\mathcal{T}_h}, \quad \forall w \in V^{DG}$$

where \mathcal{A}^N is defined by

$$(5.12) \quad \mathcal{A}^N(v, w) := \mathcal{A}(v, w) + \langle \llbracket v \rrbracket, \{\nabla_h w\} \rangle_{\mathcal{E}_h} \quad \forall v, w \in V^{DG}$$

and \mathcal{A} is still the bilinear form defined in (2.12). We note that for the NIPG-0 case we would still have a lower block triangular system similar to (4.12), but we could not localize the estimates on u^z as it was done in Lemma 4.4. However, from (5.12), (2.12), and then (5.11) we could easily have

$$|u^z|_{1,h}^2 + \langle \mathcal{SP}(\llbracket u^z \rrbracket), \mathcal{P}(\llbracket u^z \rrbracket) \rangle_{\mathcal{E}_h} = \mathcal{A}^N(u^z, u^z) = (f, u^z)_{\mathcal{T}_h}$$

that, together with the estimates (4.13) and (4.14), would still allow us to get (4.18) (or even (4.17) if strong boundary conditions were used). This, together with the known (optimal) error estimates for NIPG-0 in the DG-norm (see. e.g. [12]), would still allow to follow the lines of the proof of Theorem 5.1 and get, for an s -strongly regular decomposition

$$(5.13) \quad \|u - u_h\|_{0,\Omega} \lesssim (h^{\frac{3}{2}} + h^{1+s}) (\|f\|_{1,\Omega}^2 + \|f\|_{0,\infty,\Omega}^2)^{1/2},$$

and

$$(5.14) \quad \|u - u_h\|_{0,\Omega} \lesssim (h^2 + h^{1+s}) (\|f\|_{1,\Omega}^2 + \|f\|_{0,\infty,\Omega}^2)^{1/2}$$

if strong boundary conditions were also used. Note that, in view of Remark 4.1, the term h^{1+s} appearing in (5.13) and (5.14) requires less regular decompositions than the corresponding h^ζ appearing in [12, Theorem 8.13]. Indeed, the optimal h^2 is achieved here under the assumption (see (4.1)) $|T_1| - |T_2| \lesssim h^{d+1}$, while in [12] the assumption is $|T_1| - |T_2| \lesssim h^{3d-2}$. Finally, in order to compare with the results of [23], we point out that, according to case (ii) after Lemma 4.4, on a perfectly uniform mesh we would have $\llbracket u^z \rrbracket(m_e) = 0$ on internal edges. Hence, the term III in (5.5) would vanish identically, and the proof of Theorem 5.1 would simplify considerably.

6. L^2 ERROR ANALYSIS ON MORE GENERAL GRIDS

In this section we present a variant of the estimates of the previous section, in which we trade part of the freedom in the choice of the weights in (2.8) for weaker assumptions on the mesh (namely, just shape regularity in two dimensions and quasi-uniformity in three dimensions). We recall that a sequence $\{\mathcal{T}_h\}_h$ of decompositions is said to be *shape regular* if there exists a constant C_{SR} such that for every decomposition in the sequence and for every element T in the decomposition we have

$$(6.1) \quad h_T \leq C_{SR} \rho_T$$

where ρ_T is the radius of the biggest sphere that can be inscribed in T . On the other hand, a sequence $\{\mathcal{T}_h\}_h$ of decompositions is said to be *quasi uniform* if

there exists a constant C_{QU} such that for every decomposition in the sequence and for every pair of elements T_1 and T_2 in the decomposition we have

$$(6.2) \quad h_{T_1} \leq \rho_{T_2}$$

where again ρ_{T_2} is the radius of the biggest sphere that can be inscribed in T_2 . It is obvious that quasi uniformity implies shape regularity, but not vice-versa.

We have now the following variant of Theorem 5.1.

Theorem 6.1. *Let $\Omega \subset \mathbb{R}^d, d \geq 1$ be a convex domain. Let $f \in H^1(\Omega)$ and let u be the solution of the Poisson problem (1.1). Let \mathcal{T}_h be a shape-regular sequence of decompositions, and let $u_h \in V_h^{DG}$ be the solution of (2.14) (or, equivalently, of (4.12)). Assume moreover that $\alpha_e = \alpha$, independent of e for all internal edges, $\alpha_e = 2\alpha$ for all boundary edges and either i) $d = 2$ or ii) $d = 3$ and the decomposition is quasi-uniform, with $h_e = |e|/h_{max}$ and h_{max} is the maximum diameter of the elements in \mathcal{T}_h . Then, the following error estimate holds*

$$(6.3) \quad \|u - u_h\|_{0,\Omega} \lesssim h^2 (\|f\|_{1,\Omega}^2 + \|f\|_{0,\infty,\Omega}^2)^{1/2}.$$

Proof. We follow the proof of Theorem 5.1 up to (5.5), that we now rewrite as

$$(6.4) \quad \begin{aligned} & \|u - u_h\|_{0,\Omega}^2 \\ &= (\nabla(u - u_h), \nabla(\psi - \psi^I))_{\mathcal{T}_h} - \langle \llbracket u - u_h \rrbracket, \{\nabla(\psi - \psi^I)\} \rangle_{\mathcal{E}_h} \\ & \quad - \langle \llbracket u - u_h \rrbracket, \{\nabla\psi^I\} \rangle_{\mathcal{E}_h} \\ &=: I + II + III. \end{aligned}$$

Then we keep unchanged the estimates (5.6) and (5.7) of pieces I and II , respectively, and we restart the estimate of III , that, as in (5.8), we can write as

$$(6.5) \quad III = -\langle \mathcal{P}[\llbracket u^z \rrbracket], \{\nabla\psi^I\} \rangle_{\mathcal{E}_h}.$$

From Lemma 4.4 (and recalling that $\alpha_e = \alpha$ for internal edges and $\alpha_e = 2\alpha$ for boundary edges) we have now, for all $e \in \mathcal{E}_h$,

$$(6.6) \quad \llbracket u^z \rrbracket(m_e) \cdot \nu^e = \frac{h_e}{2\alpha|e|} \int_{\Omega} f \psi^e \, dx \quad \forall e \in \mathcal{E}_h,$$

where, however, h_e is now equal to $|e|$ (the *length* of the edge e) in two dimensions, and equal to $|e|/h_{max}$ (the *area* of the face e divided by the maximum diameter in \mathcal{T}_h) in three dimensions. We can now proceed to the estimate of III .

$$\begin{aligned} |III| &= |\langle \mathcal{P}[\llbracket u^z \rrbracket], \{\nabla\psi^I\} \rangle_{\mathcal{E}_h}| = \left| \sum_{e \in \mathcal{E}_h} \int_e \llbracket u^z \rrbracket(m_e) \cdot \{\nabla\psi^I\} \, dl \right| \\ &= \left| \sum_{e \in \mathcal{E}_h} \left(|e| \llbracket u^z \rrbracket(m_e) \cdot \nu^e \right) \left(\{\nabla\psi^I\} \cdot \nu^e \right) \right| \end{aligned}$$

$$(6.7) \quad = \left| \sum_{e \in \mathcal{E}_h} \left(\frac{h_e}{2\alpha} \int_{\Omega} f \psi^e dx \right) \{ \nabla \psi^I \} \cdot \boldsymbol{\nu}^e \right| =: \left| \int_{\Omega} f g dx \right|,$$

having set

$$(6.8) \quad g(x) := \sum_{e \in \mathcal{E}_h} \frac{h_e}{2\alpha} \{ \nabla \psi^I \} \cdot \boldsymbol{\nu}^e \psi^e(x).$$

Let \bar{f} be the piecewise constant approximation of f on \mathcal{T}_h . Then, by adding and subtracting \bar{f} , using the Cauchy-Schwarz inequality and classical approximation estimates we have:

$$(6.9) \quad \begin{aligned} \int_{\Omega} f g dx &= \int_{\Omega} (f - \bar{f}) g dx + \int_{\Omega} \bar{f} g dx \\ &\lesssim \|f - \bar{f}\|_{0,\Omega} \|g\|_{0,\Omega} \\ &\quad + \left(\sum_{T \in \mathcal{T}_h} |T| (\bar{f}|_T)^2 \right)^{1/2} \left(\sum_{T \in \mathcal{T}_h} |T|^{-1} \left(\int_T g dx \right)^2 \right)^{1/2} \\ &\lesssim h \|f\|_{1,\Omega} \|g\|_{0,\Omega} + \|\bar{f}\|_{0,\Omega} \left(\sum_{T \in \mathcal{T}_h} |T|^{-1} \left(\int_T g dx \right)^2 \right)^{1/2}. \end{aligned}$$

On the other hand we have by (6.8), (4.10), shape regularity, and usual interpolation estimates

$$(6.10) \quad \begin{aligned} \|g\|_{0,\Omega}^2 &= \sum_{T \in \mathcal{T}_h} \int_T \sum_{e \subset \partial T} \left(\frac{h_e}{2\alpha} \{ \nabla \psi^I \} \cdot \boldsymbol{\nu}^e \psi^e(x) \right)^2 \\ &\lesssim h^2 \| \nabla \psi^I \|_{0,\Omega}^2 \lesssim h^2 \| \psi \|_{2,\Omega}^2. \end{aligned}$$

In order to estimate the integral of g on T we first note that using (6.8), (4.10), and (4.4) we deduce

$$(6.11) \quad \begin{aligned} \int_T g dx &= \int_T \sum_{e \subset \partial T} \frac{h_e}{2\alpha_e} \{ \nabla \psi^I \} \cdot \boldsymbol{\nu}^e \psi^e(x) dx \\ &= \sum_{e \subset \partial T} \frac{h_e}{2\alpha} \{ \nabla \psi^I \} \cdot \boldsymbol{\nu}^e \int_T \psi^e(x) dx \\ &= \sum_{e \subset \partial T} \frac{h_e}{2\alpha} \{ \nabla \psi^I \} \cdot \boldsymbol{\nu}^e \frac{|T|}{d+1} \mathbf{n}_T^e \cdot \boldsymbol{\nu}^e \\ &= \sum_{e \subset \partial T} \frac{h_e}{2\alpha} \{ \nabla \psi^I \} \cdot \mathbf{n}_T^e \frac{|T|}{d+1}. \end{aligned}$$

Now we observe that for $d = 2$ we have $h_e = |e|$ while for $d = 3$ we assumed $h_e = |e|/h_{max}$. In *both cases* we have then

$$\begin{aligned}
 \sum_{e \subset \partial T} \frac{h_e}{2\alpha} \{\nabla \psi^I\} \cdot \mathbf{n}_T^e \frac{|T|}{d+1} &= \sum_{e \subset \partial T} \frac{|e|}{2\alpha h_{max}^{d-2}} \{\nabla \psi^I\} \cdot \mathbf{n}_T^e \frac{|T|}{d+1} \\
 (6.12) \qquad \qquad \qquad &= \frac{|T|}{2(d+1)\alpha h_{max}^{d-2}} \int_{\partial T} \{\nabla \psi^I\} \cdot \mathbf{n}_T.
 \end{aligned}$$

We then set

$$(6.13) \qquad \qquad \qquad \tilde{h}_T^2 := \frac{|T|}{2(d+1)\alpha h_{max}^{d-2}}$$

(which behaves as h_T^2 both in two and three dimensions) and then start our estimate from (6.11) and (6.12). We add and subtract ψ to ψ^I , use Cauchy-Schwarz and the divergence theorem, then (2.5) and usual interpolation estimates on the first term and Cauchy-Schwarz on the second term

$$\begin{aligned}
 \left| \int_T g \, dx \right| &= \left| \tilde{h}_T^2 \int_{\partial T} \{\nabla \psi^I\} \cdot \mathbf{n}_T \right| \\
 &= \tilde{h}_T^2 \left| \sum_{e \subset \partial T} \int_e [\{\nabla \psi^I - \nabla \psi\}] \cdot \mathbf{n}_T^e \, dl + \int_{\partial T} \nabla \psi \cdot \mathbf{n}_T \, dl \right| \\
 (6.14) \qquad \qquad \qquad &\lesssim \tilde{h}_T^2 \sum_{e \subset \partial T} |e|^{1/2} \|\{\nabla \psi^I - \nabla \psi\}\|_{0,e} + \tilde{h}_T^2 \int_T |\Delta \psi| \, dx \\
 &\lesssim \tilde{h}_T^2 \sum_{e \subset \partial T} |e|^{1/2} h^{1/2} \|\psi\|_{2,K_e} + \tilde{h}_T^2 |T|^{1/2} \|\Delta \psi\|_{0,T} \\
 &\lesssim h^{2+d/2} \sum_{e \subset \partial T} \|\psi\|_{2,K_e}.
 \end{aligned}$$

From (6.14) we have immediately

$$(6.15) \qquad \sum_{T \in \mathcal{T}_h} |T|^{-1} \left(\int_T g \, dx \right)^2 \lesssim \sum_{T \in \mathcal{T}_h} h_T^{-d} \left(\int_T g \, dx \right)^2 \lesssim h^4 \|\psi\|_{2,\Omega}^2.$$

Hence, from (6.7), (6.9), (6.10), and (6.14) we deduce

$$(6.16) \qquad \qquad \qquad |III| \lesssim h^2 \|f\|_{1,\Omega} \|\psi\|_{2,\Omega} \lesssim h^2 \|u - u_h\|_{0,\Omega}.$$

Collecting (5.6) –(5.7) and (6.16) we conclude the estimate. \square

Remark 6.1. *Our guess is that the assumption of Theorem 6.1 on the choice of the penalty parameters α_e is just a technical one, and that the result could be obtained under more general assumptions. However, we did not thoroughly investigate this matter.*

7. NUMERICAL EXPERIMENTS

In this section we present some numerical experiments that validate the analysis for the IIPG-0 discretization. Moreover, some tests are devoted to compare, at least in a simple test case, the performance of the IIPG-0 and IIPG methods. For completeness, we also provide comparison with the Symmetric Interior Penalty method (SIPG [3]) and its weakly penalized version, SIPG-0. The non-symmetric Interior Penalty method (NIPG [19, 20]), and its weakly penalized version, were also considered. However, as the results are very similar to those obtained with the IIPG and IIPG-0 methods, to keep the clarity of the graphics we have chosen not to report them here.

The experiments are performed with a simple test case on the unit square $\Omega = (0, 1)^2$, using piecewise linear approximations on triangular grids. The forcing term f is chosen so that the analytical solution of (1.1) is given by $u(x, y) = \sin(2\pi x) \sin(2\pi y)$. All the experiments were run with two different choices of the parameter α_e in (2.8). The simplest choice is $\alpha_e = \alpha$, constant on all the edges; the second one, in agreement with the assumptions of Theorem 6.1, corresponds to choose $\alpha_e = \alpha$, constant on the internal edges, and $\alpha_e = 2\alpha$ on the boundary edges. We also considered two types of grids, structured (hence verifying the assumptions of Theorem 5.1), and unstructured (see Fig. 7.1). The results were, as expected, the same.

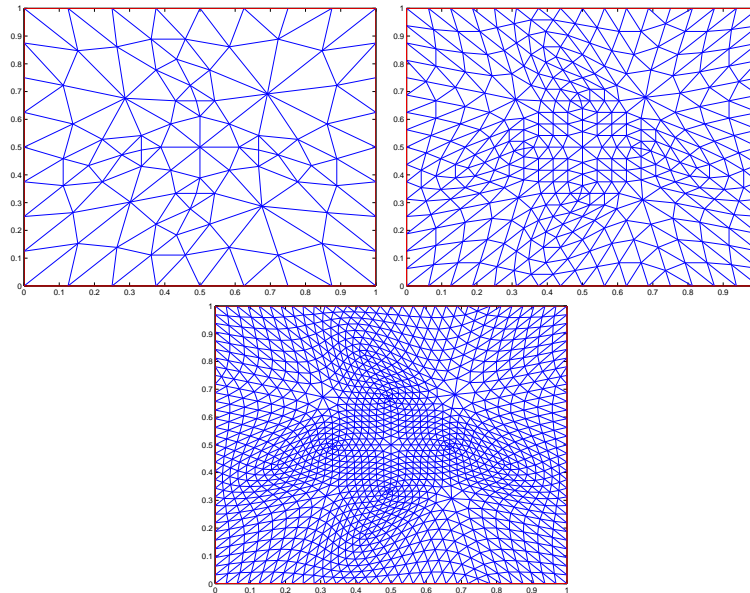


FIGURE 7.1. Unstructured meshes used in the computations: the coarsest mesh (left figure); first refinement (center) and second refinement (right figure).

In Fig. 7.2 we study the convergence of the IIPG and IIPG-0 methods in several norms on structured meshes with $\alpha_e = 5$ on all the edges. We are therefore in the assumptions of Theorem 5.1, and not in the assumptions of Theorem 6.1. From the graphics it can be seen that both methods attain second order convergence in the L^2 -norm (left diagram), and first order in the $\|\cdot\|_{DG}$ -norm (right diagram). As it should be expected, in the “jump”-seminorm $|\cdot|_*$ the original IIPG method outperforms the IIPG-0 method. However, since the error in the H^1 -broken seminorm $|\cdot|_{1,h}$ is the dominant term in the error $\|u - u_h\|_{DG}$ (which is somehow natural since the exact solution is very smooth), both methods produce approximation with the same accuracy in this norm.

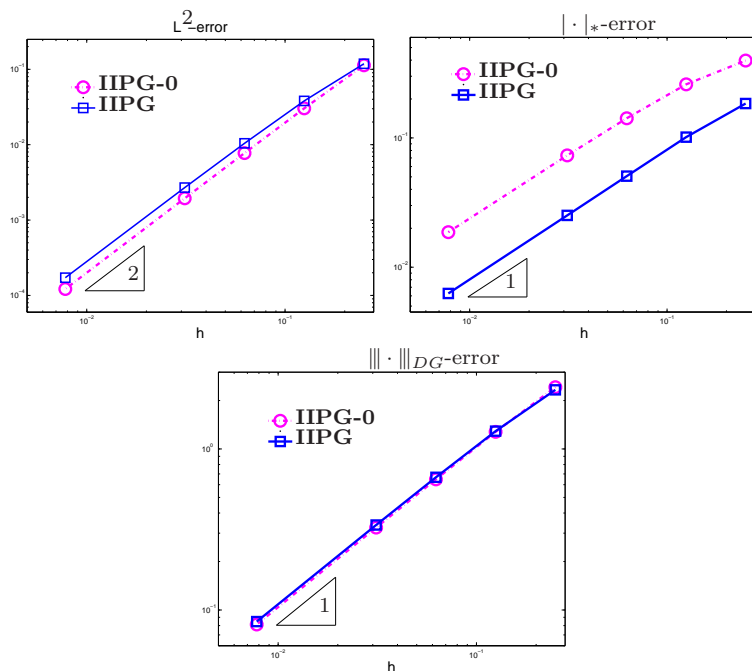


FIGURE 7.2. Convergence diagrams on structured meshes for IIPG and IIPG-0 (with $\alpha_e = 5$ on all the edges) in several norms: L^2 -norm (left); $|\cdot|_*$ seminorm (center), and $\|\cdot\|_{DG}$ -norm (right).

In Fig. 7.3 we represent the convergence diagrams on unstructured meshes, with $\alpha_e = 5$ on internal edges, and $\alpha_e = 10$ on the boundary edges, thus verifying the assumptions of Theorem 6.1, and not, in a sense, those of Theorem 5.1. Here, together with IIPG and IIPG-0, we consider also SIPG, SIPG-0. In the graphics of Fig. 7.3, (as well as in Fig. 7.4), the original IP methods are represented with continuous line, and the corresponding IP-0 methods with dashed lines. More precisely, IIPG is represented by $-\square-$; IIPG-0 by $-\cdot-\circ-\cdot-$; SIPG by $-\triangle-$, and SIPG-0 by $-\cdot-\nabla-\cdot-$.

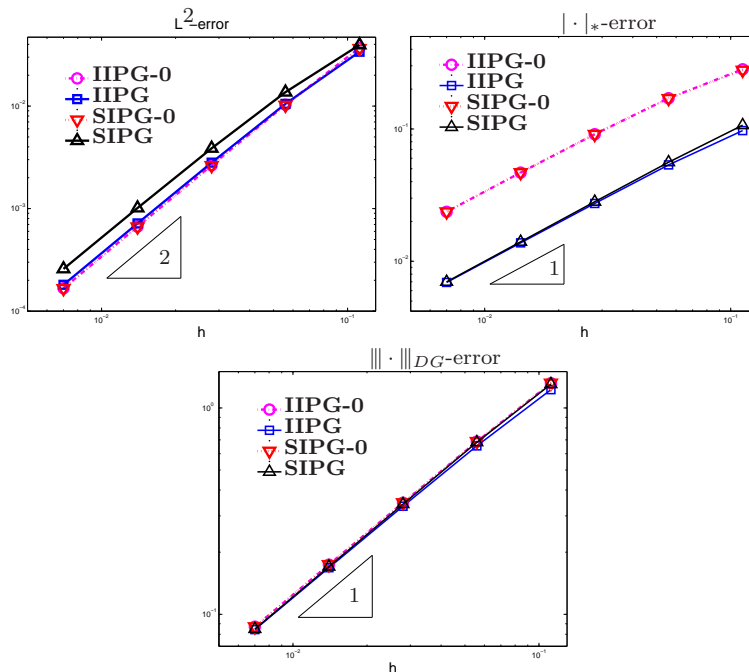


FIGURE 7.3. Convergence diagrams on unstructured meshes for IIPG, IIPG-0, SIPG and SIPG-0 (with $\alpha_e = 5$ on $e \in \mathcal{E}_h^\circ$ and $\alpha_e = 10$ on $e \in \mathcal{E}_h^\partial$) in several norms: L^2 -norm (left); $|\cdot|_*$ semi-norm (center); $|||\cdot|||_{DG}$ -norm (right).

It can be seen that all the methods show second-order convergence in L^2 , and first-order convergence in the DG-norm. It can also be observed that all the weakly penalized methods give slightly smaller errors than the corresponding original ones in the L^2 -norm. As it happened before, in the $|\cdot|_*$ -seminorm the approximations with the original IP methods are clearly more accurate.

Finally, we ran the same test with $\alpha_e = 5$ on all edges, thus violating the hypotheses of Theorem 6.1. In a sense, from the practical point of view we may say that the meshes of Fig. 7.1 are not 1-strongly regular (see definition (4.1)), and therefore also Theorem 5.1 does not apply directly. However, the results are the same also in this case (see Fig. 7.4).

This could be interpreted in two possible ways. From the one hand, as already pointed out in Remark 6.1, the hypothesis of Theorem 6.1 on the α_e is purely technical. On the other hand, when using a sequence of uniform refinements of a given coarse mesh we are approaching, asymptotically, the situation of 1-strongly regular meshes, as the number of interelement edges where the condition is *not* satisfied grows like $O(h)$ whereas the total number of internal edges grows like $O(h^2)$.

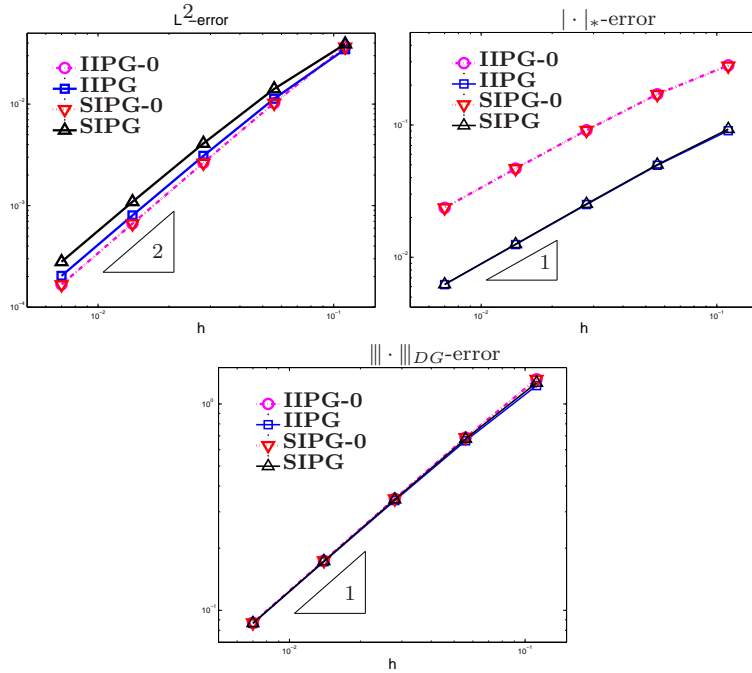


FIGURE 7.4. Convergence diagrams on unstructured meshes for IIPG, IIPG-0, SIPG and SIPG-0 (with $\alpha_e = 5$ on all the edges) in several norms: L^2 -norm (left); $|\cdot|_*$ semi-norm (center); $|||\cdot|||_{DG}$ -norm (right).

7.1. Sharpness of the optimal L^2 -estimate: a counterexample. We finally present a simple numerical experiment demonstrating that the regularity of the right-hand side f assumed in our analysis (and more precisely in (5.1)) is somehow necessary to obtain optimal L^2 -order of convergence. We recall that in general, see e.g. [4], one expects an L^2 estimate of the form

$$(7.1) \quad \exists C > 0 \quad \text{such that} \quad \forall h > 0, \forall f \in L^2(\Omega) \quad \|u(f) - u_h(f)\|_{0,\Omega} \leq Ch^2 \|f\|_{0,\Omega},$$

where $u(f)$ and $u_h(f)$ are the exact and (respectively) the approximate solution of our problem (1.1) having f as right-hand side. The aim of this section is to give numerical evidence that denies (7.1) for all the non symmetric methods IIPG, IIPG-0, NIPG, and NIPG-0. We consider a simple one-dimensional example on the unit interval $[0, 1]$:

$$(7.2) \quad -u_{xx} = f \quad \text{in } [0, 1], \quad u = 0 \quad \text{at } \{0\} \text{ and } \{1\}.$$

We start by noting that in one-dimension the two methods IIPG and IIPG-0 coincide, and hence produce the same approximate solutions. In a similar way NIPG and NIPG-0 also coincide. Hence in what follows we will simply refer

to IIPG and NIPG. We also included for comparison the corresponding results obtained with the SIPG discretizations. We aim at showing that for the IIPG and NIPG approximations it holds:

$$\forall C_0 > 0 \quad \exists f \in L^2([0, 1]) \quad \text{and} \quad \exists h > 0, \quad \text{s.t.} \\ \|u(f) - u_h(f)\|_0 > C_0 h^2 \|f\|_0.$$

Actually, we will show something a bit stronger. Namely, we show that

$$(7.3) \quad \forall C_0 > 0 \quad \forall h > 0 \quad \exists f^* = f^*(h) \in L^2([0, 1]) \quad \text{s.t.} \\ \mathcal{Q}_2 := \frac{\|u(f^*) - u_h(f^*)\|_0}{h^2 \|f^*\|_0} > C_0.$$

In particular, we will show that the quotient \mathcal{Q}_2 grows linearly as h decreases, and cannot be uniformly bounded, contrary to the behavior of the SIPG. In other words:

$$(7.4) \quad \begin{aligned} \mathcal{Q}_2^{IIPG}(h, f^*(h)) &\longrightarrow \infty \quad \text{as} \quad h \rightarrow 0, \\ \mathcal{Q}_2^{NIPG}(h, f^*(h)) &\longrightarrow \infty \quad \text{as} \quad h \rightarrow 0, \\ \mathcal{Q}_2^{SIPG}(h, f^*(h)) &\simeq 1. \end{aligned}$$

Moreover, we will show that *for the above f^* 's and for the corresponding solutions $u(f^*)$ and approximate solutions $u_h(f^*)$* one has instead the following experimental behavior, clearly suggesting first order convergence in L^2 :

$$(7.5) \quad \exists C_1 > 0, \quad \text{s.t.} \quad \lim_{h \rightarrow 0} \mathcal{Q}_1(h, f^*(h)) \equiv \lim_{h \rightarrow 0} \frac{\|u(f^*) - u_h(f^*)\|_0}{h \|f^*\|_0} = C_1.$$

We now describe the numerical test. We take for \mathcal{T}_h a family of uniform partitions of $[0, 1]$ with mesh size $h = 3^{-1}2^{-k}$, and $k = 2, 3, \dots, 12$. Associated to each mesh we construct a family of functions $\{f^*(h)\}$. Each f^* is a piecewise linear polynomial on each mesh:

$$f^*(h) = \begin{cases} -\frac{(x-x_i)}{h} & 0 \leq x_i < x < x_{i+1} \leq 1/4, \\ \frac{(x-x_i)}{h} & 1/4 \leq x_i < x < x_{i+1} \leq 3/4, \\ -\frac{(x-x_i)}{h} & 3/4 \leq x_i < x < x_{i+1} \leq 1, \end{cases}$$

where x_i are the nodes and $h = x_{i+1} - x_i$. The corresponding exact solution $u(f^*)$ of the problem (7.2) (with right hand side f^*) is computed analytically. Fig. 7.5 shows f^* (top figures) and the corresponding exact solutions $u(f^*)$ (bottom figures) for the first three uniform meshes used in the computations. Clearly f^* is in $L^2([0, 1])$ (and actually also in $L^\infty([0, 1])$) but $f^* \notin H^1([0, 1])$. We wish to stress

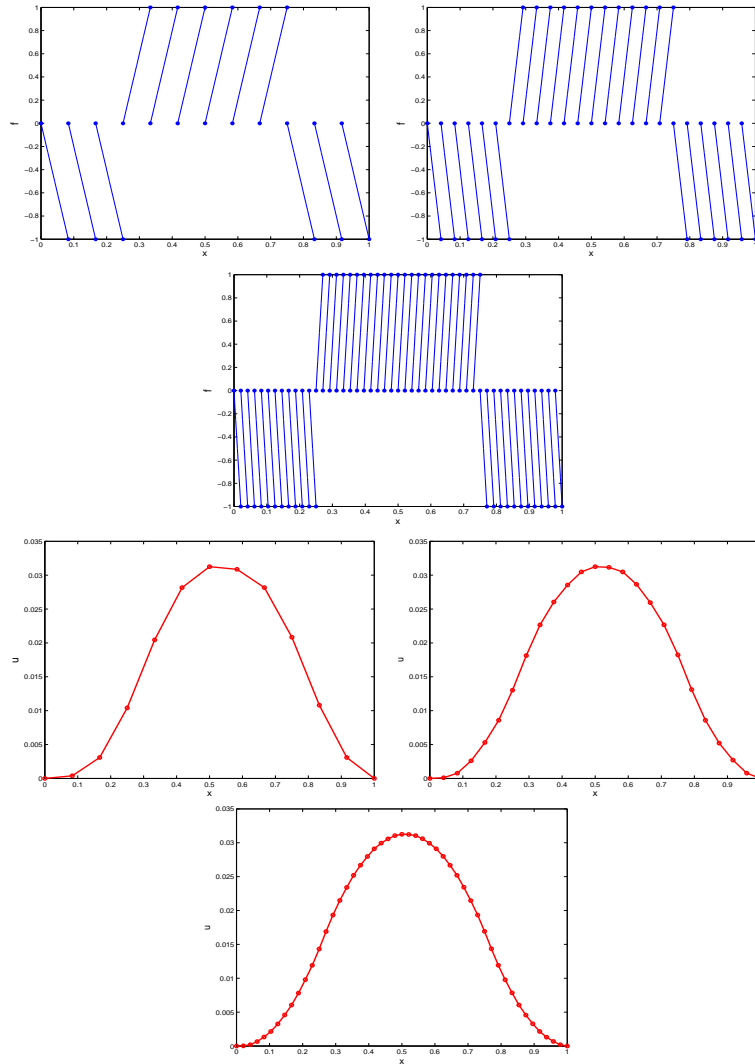


FIGURE 7.5. Graphic representations of $f^*(h)$ (top figures) and the corresponding exact solution $u(f^*)$ (bottom figures), computed on uniform meshes with mesh size $h = 1/12$ (left figures), $h = 1/24$ (center) and $h = 1/48$ (rightmost figures).

that both the L^2 -norm and the L^∞ -norm of $f^*(h)$ are actually independent of h :

$$\|f^*(h)\|_{L^2([0,1])} = \frac{1}{\sqrt{3}} \quad \|f^*(h)\|_{L^\infty([0,1])} = 1.$$

The convergence diagrams in the L^2 -norm for all the methods are given in Fig. 7.6. For the IIPG and NIPG methods, only first order is attained, while SIPG converges with second order, as expected from the classical theory [3, 4]

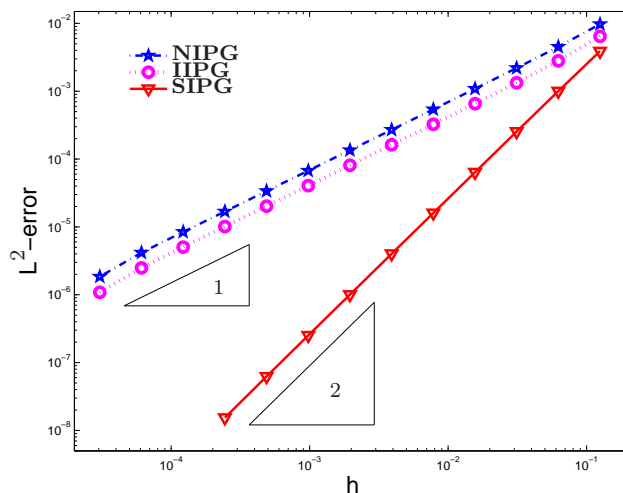


FIGURE 7.6. Convergence diagrams in the L^2 -norm. The IIPG method is represented by $\cdots \circ \cdots$; the NIPG by $-\cdot-\star-\cdot-\cdot-$, and the SIPG by $-\nabla-$.

together with the regularity of the test problem, $f \in L^2([0, 1])$.

To verify (and support) numerically the statements (7.3)–(7.5), we have represented in a log-log scale the values of the (error constants) quotients \mathcal{Q}_2 and \mathcal{Q}_1 defined in (7.3) and in (7.5), respectively, together with the quotient

$$\mathcal{Q}_{1/2} := \frac{\|u(f^*) - u_h(f^*)\|_0}{h^{1/2}\|f^*\|_0}.$$

Since all the methods are at least first order convergent in L^2 (see [4]), we clearly expect $\mathcal{Q}_{1/2} \rightarrow 0$ as $h \rightarrow 0$. This can indeed be seen in Fig. 7.7, where the diagrams for the three methods are depicted. Observe that the behavior predicted in (7.4) for \mathcal{Q}_2 can be easily checked in the graphics. While for the SIPG method it remains constant, for the IIPG and NIPG methods it increases linearly as h decreases. In contrast, \mathcal{Q}_1 remains constant for IIPG and NIPG methods, which confirms (7.5) and supports our conclusion that the methods are at most first order convergent if the data f is only in L^2 . In Table 7.1 we also report the computed values of the quotients \mathcal{Q}_2 (left table) and \mathcal{Q}_1 (right table).

All the experiments have been carried out with MATLAB on a Mac-Book Pro with 8Gb of Ram memory.

Remark 7.1. *One might argue about our construction of the numerical test, since the L^2 -suboptimality is demonstrated for a sequence of mesh dependent functions $f^*(h)$. Indeed we showed (numerically) (7.3) rather than producing the most*

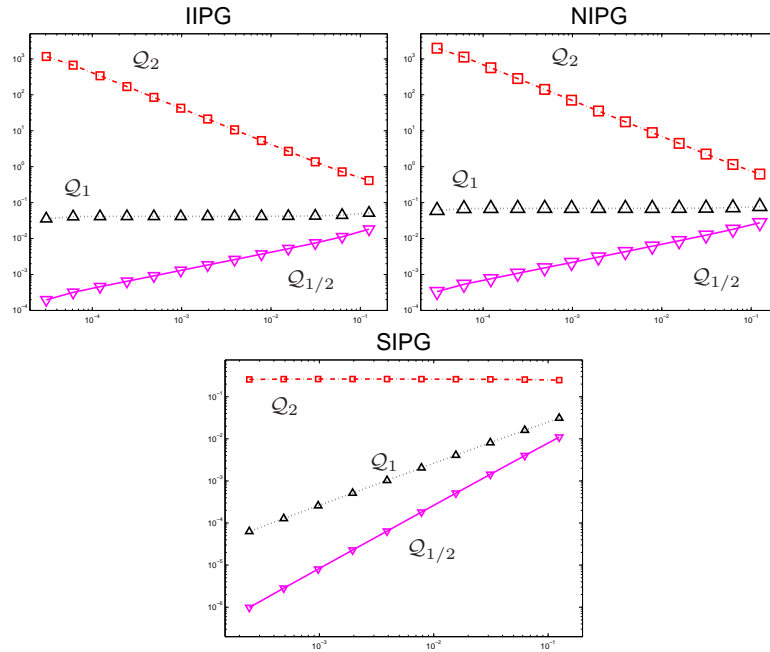


FIGURE 7.7. Lower bounds for the error best constants: \mathcal{Q}_2 ($- \cdot - \square - \cdot -$), \mathcal{Q}_1 ($\cdot \cdot \triangle \cdot \cdot$), and $\mathcal{Q}_{1/2}$ ($- \nabla -$) as functions of the mesh size, for IIPG (left), NIPG (center), and SIPG (right).

common type of (numerical) counterexample:

(7.6) $\exists f^* \in L^2([0, 1])$ such that not

$$\left\{ \exists C_0 > 0 \quad \forall h > 0 \quad \frac{\|u(f^*) - u_h(f^*)\|_0}{\|f^*\|_0} < C_0 h^2 \right\}.$$

However we point out that, in the first place, (7.3) easily implies the falseness of (7.1) and hence it must be considered as a legitimate counterexample. Moreover, using the uniform boundedness principle (also known as Banach-Steinhaus theorem², see for instance [21, Theorem 2.5 & 2.6]) it is not difficult to see that (7.3) actually implies (7.6). More precisely, we can define a family of linear and continuous operators $E_h : L^2([0, 1]) \longrightarrow L^2([0, 1])$ by

$$(7.7) \quad E_h(f) := h^{-2}(u(f) - u_h(f)) \quad \forall f \in L^2([0, 1]),$$

²Uniform boundedness principle : let X, Y be two Banach spaces, let $\{E_h\}$ be a collection of continuous linear mappings $E_h : X \longrightarrow Y$ and let $\|\cdot\|_{\mathcal{L}(X, Y)}$ denote the operator norm.

$$\text{if } \sup_h \|E_h x\|_Y < \infty, \quad \forall x \in X \quad \implies \quad \sup_h \|E_h\|_{\mathcal{L}(X, Y)} < \infty.$$

$$(a) \text{ Computed } \mathcal{Q}_2 = \frac{\|u(f^*) - u_h(f^*)\|_0}{h^2 \|f^*\|_0}$$

$$(b) \mathcal{Q}_1 = \frac{\|u(f^*) - u_h(f^*)\|_0}{h \|f^*\|_0}$$

N	SIPG	IIPG	NIPG	N	IIPG	NIPG
12	0.4039	0.66	0.49	12	0.16404	0.12277
24	0.4311	0.71	1.08	24	0.08921	0.13501
48	0.4440	1.24	2.00	48	0.07756	0.12508
96	0.4503	2.36	3.90	96	0.07381	0.12173
192	0.4534	4.65	7.71	192	0.07257	0.12052
384	0.4549	9.23	15.36	384	0.07212	0.12004
768	0.4557	18.42	30.68	768	0.07194	0.11983
1536	0.4560	36.80	61.30	1536	0.07186	0.11973
3072	0.4566	73.54	122.56	3072	0.07182	0.11969
6144	0.4540	147.05	245.07	6144	0.07180	0.11966
12288	0.4465	294.14	490.17	12288	0.07181	0.11967

TABLE 7.1. Numerical Computed values of the quotients \mathcal{Q}_2 (left table) and \mathcal{Q}_1 (right table).

and we denote with $\|E_h\|_{\mathcal{L}(L^2[0,1],L^2[0,1])}$ its norm. Then (7.3) implies that

$$\sup_h \|E_h\|_{\mathcal{L}(L^2[0,1],L^2[0,1])} = +\infty,$$

that is just the negation of the **thesis** of the uniform boundedness principle. Therefore we conclude that E_h does not satisfy the hypothesis of the Theorem and therefore

$$\exists f \in L^2([0,1]) \quad \forall C > 0 \quad \exists h > 0 \text{ such that } \|E_h(f)\|_{L^2[0,1]} > C,$$

that is exactly (7.6)

ACKNOWLEDGMENTS

Blanca Ayuso is grateful to Doug Arnold, from IMA (Minneapolis) for fruitful discussions. The authors thank J.Xu from Penn-State for suggesting the use of 1-strongly regular meshes. Part of this work was completed while the first author was visiting IMATI-CNR of Pavia in November-December 2009 and July 2010. She is grateful to the IMATI for the kind hospitality. She was partially supported by MEC under project MTM2008 – 03541. The second and fourth authors were

partially supported by the Italian MIUR through the project PRIN2008. All the authors except the third were partially supported by Azione Integrata Spagna-Italia IT097ABB10 (Italian MIUR) and HI2008 – 0173 (Spanish MEC).

REFERENCES

- [1] R. A. Adams. *Sobolev spaces*. Academic Press [A subsidiary of Harcourt Brace Jovanovich, Publishers], New York-London, 1975. Pure and Applied Mathematics, Vol. 65.
- [2] S. Agmon. *Lectures on elliptic boundary value problems*. Prepared for publication by B. Frank Jones, Jr. with the assistance of George W. Batten, Jr. Van Nostrand Mathematical Studies, No. 2. D. Van Nostrand Co., Inc., Princeton, N.J.-Toronto-London, 1965.
- [3] D. N. Arnold. An interior penalty finite element method with discontinuous elements. *SIAM J. Numer. Anal.*, 19(4):742–760, 1982.
- [4] D. N. Arnold, F. Brezzi, B. Cockburn, and L. D. Marini. Unified analysis of discontinuous Galerkin methods for elliptic problems. *SIAM J. Numer. Anal.*, 39(5):1749–1779 (electronic), 2001/02.
- [5] B. Ayuso de Dios and L. Zikatanov. Uniformly convergent iterative methods for discontinuous Galerkin discretizations. *J. Sci. Comput.*, 40(1-3):4–36, 2009.
- [6] R. E. Bank and J. Xu. Asymptotically exact a posteriori error estimators. I. Grids with superconvergence. *SIAM J. Numer. Anal.*, 41(6):2294–2312 (electronic), 2003.
- [7] S. C. Brenner. Poincaré-Friedrichs inequalities for piecewise H^1 functions. *SIAM J. Numer. Anal.*, 41(1):306–324 (electronic), 2003.
- [8] S. C. Brenner and L. Owens. A weakly over-penalized non-symmetric interior penalty method. *JNAIAM J. Numer. Anal. Ind. Appl. Math.*, 2(1-2):35–48, 2007.
- [9] S. C. Brenner, L. Owens, and L.-Y. Sung. A weakly over-penalized symmetric interior penalty method. *Electron. Trans. Numer. Anal.*, 30:107–127, 2008.
- [10] F. Brezzi, B. Cockburn, L. D. Marini, and E. Süli. Stabilization mechanisms in discontinuous Galerkin finite element methods. *Comput. Methods Appl. Mech. Engrg.*, 195(25-28):3293–3310, 2006.
- [11] F. Brezzi, T. J. R. Hughes, L. D. Marini, and A. Masud. Mixed discontinuous Galerkin methods for Darcy flow. *J. Sci. Comput.*, 22/23:119–145, 2005.
- [12] E. Burman and B. Stamm. Low order discontinuous Galerkin methods for second order elliptic problems. *SIAM J. Numer. Anal.*, 47(1):508–533, 2008/09.
- [13] H. Chen. Superconvergence properties of discontinuous Galerkin methods for two-point boundary value problems. *Int. J. Numer. Anal. Model.*, 3(2):163–185, 2006.
- [14] P. G. Ciarlet. Basic error estimates for elliptic problems. In *Handbook of numerical analysis, Vol. II*, Handb. Numer. Anal., II, pages 17–351. North-Holland, Amsterdam, 1991.
- [15] V. Dolejší and O. Havle. The L^2 -optimality of the IIPG method for odd degrees of polynomial approximation in 1D. *J. Sci. Comput.*, 42(1):122–143, 2010.
- [16] J. Guzmán and B. Rivière. Sub-optimal convergence of non-symmetric discontinuous Galerkin methods for odd polynomial approximations. *J. Sci. Comput.*, 40(1-3):273–280, 2009.
- [17] M. G. Larson and A. J. Niklasson. Analysis of a family of discontinuous Galerkin methods for elliptic problems: the one dimensional case. *Numer. Math.*, 99(1):113–130, 2004.
- [18] Q. Lin and J. Xu. Linear finite elements with high accuracy. *J. Comput. Math.*, 3(2):115–133, 1985.
- [19] B. Rivière, M. F. Wheeler, and V. Girault. Improved energy estimates for interior penalty, constrained and discontinuous Galerkin methods for elliptic problems. I. *Comput. Geosci.*, 3(3-4):337–360 (2000), 1999.

- [20] B. Rivière, M. F. Wheeler, and V. Girault. A priori error estimates for finite element methods based on discontinuous approximation spaces for elliptic problems. *SIAM J. Numer. Anal.*, 39(3):902–931 (electronic), 2001.
- [21] W. Rudin. *Functional analysis*. McGraw-Hill Book Co., New York, 1973. McGraw-Hill Series in Higher Mathematics.
- [22] S. Sun and M. F. Wheeler. Symmetric and nonsymmetric discontinuous Galerkin methods for reactive transport in porous media. *SIAM J. Numer. Anal.*, 43(1):195–219 (electronic), 2005.
- [23] K. Wang, H. Wang, S. Sun, and M. F. Wheeler. An optimal-order L^2 -error estimate for nonsymmetric discontinuous Galerkin methods for a parabolic equation in multiple space dimensions. *Comput. Methods Appl. Mech. Engrg.*, 198(27-29):2190–2197, 2009.
- [24] M. F. Wheeler. An elliptic collocation-finite element method with interior penalties. *SIAM J. Numer. Anal.*, 15(1):152–161, 1978.

B. AYUSO DE DIOS
 CENTRE DE RECERCA MATEMATICA
 UAB SCIENCE FACULTY
 08193 BELLATERRA, BARCELONA, SPAIN

F. BREZZI
 IMATI DEL CNR
 VIA FERRATA 1
 27100 PAVIA, ITALY
 AND
 ISTITUTO UNIVERSITARIO DI STUDI SUPERIORI
 V.LE LUNGO TICINO SFORZA 56
 27100, PAVIA, ITALY

O. HAVLE
 FACULTY OF MATHEMATICS AND PHYSICS
 CHARLES UNIVERSITY
 PRAGUE, CZECH REPUBLIC

L. DONATELLA MARINI
 DIPARTIMENTO DI MATEMATICA
 UNIVERSITÀ DI PAVIA
 VIA FERRATA 1
 27100 PAVIA, ITALY
 AND
 IMATI DEL CNR
 VIA FERRATA 1
 27100 PAVIA, ITALY